IOP Publishing | Society for Radiological Protection Journal of Radiological Protection
J. Radiol. Prot. **39** (2019) 783–793 (11pp) https://doi.org/10.1088/1361-6498/ab23cc

Assessment of patient dose and noise level of clinical CT images: automated measurements

Choirul Anam[1,6], Wahyu Setia Budi[1], Kusworo Adi[1], Heri Sutanto[1], Freddy Haryanto[2], Mohd Hanafi Ali[3], Toshioh Fujibuchi[4] and Geoff Dougherty[5]

[1] Department of Physics, Faculty of Mathematics and Natural Sciences, Diponegoro University, Jl. Prof. Soedarto SH, Tembalang, Semarang 50275, Central Java, Indonesia
[2] Department of Physics, Faculty of Mathematics and Natural Sciences, Bandung Institute of Technology, Ganesha 10, Bandung 40132, West Java, Indonesia
[3] Department of Medical Radiation Sciences, University of Sydney, Sydney, Australia
[4] Department of Health Sciences, Faculty of Medical Sciences, Kyushu University, 3-1-1 Maidashi, Higashi-ku, Fukuoka 812-8582, Japan
[5] Department of Applied Physics and Medical Imaging, California State University Channel Islands, Camarillo, CA 93012, United States of America

E-mail: anam@fisika.undip.ac.id

Received 9 April 2019, revised 15 May 2019
Accepted for publication 22 May 2019
Published 5 July 2019

Abstract

We investigated comparisons between patient dose and noise in pelvic, abdominal, thoracic and head CT images using an automatic method. 113 patient images (37 pelvis, 34 abdominal, 25 thoracic, and 17 head examinations) were retrospectively and automatically examined in this study. Water-equivalent diameter (Dw), size-specific dose estimates (SSDE) and noise were automatically calculated from the center slice for every patient image. The Dw was calculated based on auto-contouring of the patients' edges, and the SSDE was calculated as the product of the volume CT dose index (CTDIvol) extracted from the Digital Imaging and Communications in Medicine (DICOM) header and the size conversion factor based on the Dw obtained from AAPM 204. The noise was automatically measured as a minimum standard deviation in the map of standard deviations. A square region of interest of about 1 cm^2 was used in the automated noise measurement. The SSDE values for the pelvis, abdomen, thorax, and head were 21.8 $\pm$ 7.3 mGy, 22.0 $\pm$ 4.5 mGy, 21.5 $\pm$ 4.7 mGy, and 65.1 $\pm$ 1.7 mGy, respectively. The SSDEs for the pelvis, abdomen, and thorax

[6] Author to whom any correspondence should be addressed.

0952-4746/19/030783+11$33.00 Printed in the UK

increased linearly with increasing Dw, and for the head with constant tube current, the SSDE decreased with increasing Dw. The noise in the pelvis, abdomen, thorax, and head were 5.9 ± 1.5 HU, 5.2 ± 1.4 HU, 4.9 ± 0.8 HU and 3.9 ± 0.2 HU, respectively. The noise levels for the pelvis, abdomen, and thorax of the patients were relatively constant with Dw because of tube current modulation. The noise in the head image was also relatively constant because Dw variations in the head are very small. The automated approach provides a convenient and objective tool for dose optimizations.

Keywords: automated noise calculation, automated size-specific dose estimate (SSDE), water-equivalent diameter, CT dose optimization, ALARA principle

(Some figures may appear in colour only in the online journal)

1. Introduction

Computed tomography (CT) is a powerful modality in medical imaging [1, 2] and its use continues to increase as a result of ongoing advances in its technology. However, the growing use of CT has increased the potential radiation risk to the population [3], since the dose from CT scans is greater than from other imaging modalities [4]. It was reported that the contribution from CT doses was more than half of the dose from all other radiological modalities [5]. Recently, several publications reported that there was a positive relationship between CT examinations and the subsequent occurrence of cancer [6, 7]. Therefore it is crucial to implement CT dose optimization based on the principle of as low as reasonably achievable (ALARA). In the ALARA principle, the intended purpose of the application of radiation in medical examinations is dose optimization, not simply dose reduction [8, 9]. In dose optimization, image quality with a level adequate for diagnosis should be obtained, and based on this image quality level, an image is then produced with the lowest possible dose.

For radiation dose optimization, there are two types of variables that should be considered: controllable and uncontrollable variables [10]. Controllable variables are input imaging variables such as tube voltage, tube current, gantry speed, mode of operation, pitch, slice thickness, type of reconstruction filter, modulation parameters, field of view, etc. Uncontrollable variables are directly related to the patient such as patient size, patient geometry, and attenuation of the scanned body. All these variables affect the dose and the image quality [11]. Thus, the application of the ALARA principle requires the quantification of specific quantities, such as radiation dose and image quality, for each patient personally and cannot be sufficiently represented by standardized phantoms.

Comparison between radiation doses and image quality has been investigated in previous studies [12, 13], however the studies have several limitations. The dose metric used is based on volume CTDI (CTDIvol) [12, 14], which only characterizes the output dose of CT scanner and does not take into account the size of the patient [13]. As already mentioned, the noise for the same exposure factor is strongly influenced by the size of the patient [15]. For the quantification of radiation doses in CT, a recently developed metric, the size-specific dose estimate (SSDE), has been specifically designed to take into account the individual size of each patient [16–19]. SSDE is a development of the quantification of previous doses indices that were based on standardized phantoms, such as the CTDIvol [20–23].

Another limitation is that the measurement of patient dose and noise is carried out manually [12, 13]. This approach is rather subjective and a more objective comparison between

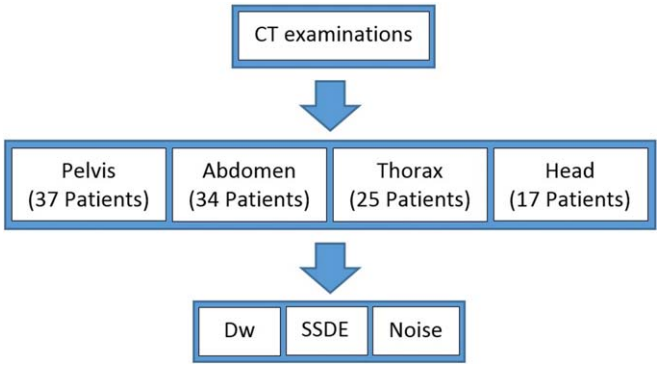

Figure 1. Schematic diagram of the current study.

patient dose and patient noise needs to be performed with an automated approach. Presently, an automated calculation of patient dose (SSDE) is already available [20, 24]. Christianson *et al* [20] developed an algorithm for automatically calculating SSDE based on an effective diameter (Deff) and more recently Anam *et al* [24] developed software for automatic SSDE based on water-equivalent diameter (Dw) [25, 26]. Recently, Christianson *et al* [27] developed a technique for automatically measuring the noise in abdominal clinical CT images. More recently, Anam *et al* [28] developed a refined automated technique for calculating noise from patient images that can be applied to all body regions, such as the head, chest, abdomen and pelvis. This opens up the opportunity to optimize patient dose more objectively, efficiently, and conveniently. However, to date, a comparison between the automatic dose and noise measurements for dose optimization purposes has never been conducted. This current study aims to implement the automated patient dose and noise in clinical images as dose optimization for the most common types of CT examinations: pelvis, abdominal, thorax and head.

2. Methods

2.1. Study design

A schematic diagram of the current study is shown in figure 1. The study was a retrospective study on 113 patient images in four CT examinations (pelvis, abdomen, thoracic and head). The number of patients were 37, 34, 25 and 17 for pelvic, abdominal, thoracic and head CT examinations. All images of patient were obtained using a MSCT Toshiba Aquilion-128, with 120 kVp and a slice thickness of 2 mm. The pitch of 0.938 for the pelvis, 1.438 for the abdomen and thorax, and 0.688 for the head, and the rotation times were 500 ms for the pelvis, abdomen, and thorax, and 750 ms for the head. The tube current modulation (TCM) technique was implemented in pelvis, abdomen and thorax examinations, and a fixed tube current (FTC) technique of 300 mA was used in the head examination. In the head examinations, constant tube current or FTC was usually employed due to the very small head size variation of the adult patients [29].

The Dw, SSDE and noise calculations were automatically calculated using one image of the middle slice (e.g. the orbitals (head), sacrum (pelvis), umbilicus (abdomen), and xiphoid process (thorax)). The SSDEs and noises for each examination were then compared as a function of Dw. Comparisons of SSDE values and noises were also shown using boxplot graphics.

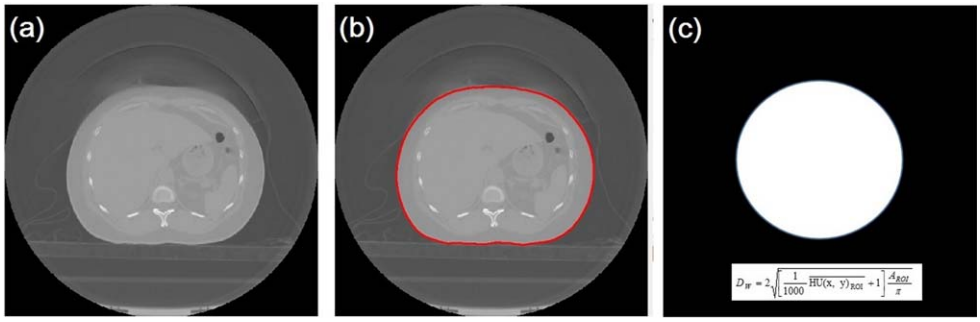

Figure 2. Steps of automated Dw calculation. (a) Image of patient, (b) result of auto-contouring of the image, (c) water-equivalent diameter (Dw) based on the result of auto-contouring.

2.2. Algorithm of automated Dw and SSDE calculations

The water-equivalent diameter (Dw) is a characterization of patient size and is the 'gold standard' metric for patient size [30]. The Dw does not only surrogate the geometrical size of the patient, but it also the attenuation characteristics [31, 32]. Automated Dw calculation was adopted from the previous study [24]. The steps in the automated Dw calculation are shown in figure 2. The calculation was started with automated patients contouring. Dw was calculated using equation:

$$\mathrm{Dw} = 2\sqrt{\left(\frac{1}{1000}\overline{\mathrm{HU}(x,\,y)_{\mathrm{ROI}}} + 1\right)\frac{A_{\mathrm{ROI}}}{\pi}}. \tag{1}$$

The region of interest (ROI) was a result of automated patient contouring. A_{ROI} was the area of the patient and $\overline{\mathrm{HU}(x,\,y)_{\mathrm{ROI}}}$ was the average HU value within the patient. Anam *et al* [24] reported that the percentage differences between the automated and the manual Dw calculations were less than 0.5%.

A metric for characterizing patient dose estimates is the size-specific dose estimate (SSDE) [32]. The SSDE values were calculated automatically based on the results of automated Dw calculations [24]. The equations to calculate the SSDE based on head and body PMMA phantoms were obtained from four different research groups organized by the American Association of Physicists in Medicine (AAPM) in 2011 [33]. The four groups used different methods, i.e. physical measurements using an anthropomorphic phantom, physical measurements using cylindrical PMMA phantoms, Monte Carlo measurements on voxelized phantoms, and Monte Carlo measurements on simple cylindrical phantoms [33]. All data were then combined to produce the equations for calculating SSDEs taking into account the patient size. The results from the four different studies were highly correlated with a R^2 of 0.942 [33]. The equation for SSDE for the pelvis, abdominal and thoracic examinations was:

$$\mathrm{SSDE} = \mathrm{CTDI}_{\mathrm{vol}}^{32} \times 4.378094 \times e^{-0.04331124 \times \mathrm{Dw}}. \tag{2}$$

The equation for SSDE for the head examinations was:

$$\mathrm{SSDE} = \mathrm{CTDI}_{\mathrm{vol}}^{16} \times 1.874799 \times e^{-0.03871313 \times \mathrm{Dw}}. \tag{3}$$

$\mathrm{CTDI}_{\mathrm{vol}}^{32}$ is the metric of CT output dose measured using 32 cm PMMA phantom, and $\mathrm{CTDI}_{\mathrm{vol}}^{16}$ is measured using 16 cm PMMA phantom. The values of $\mathrm{CTDI}_{\mathrm{vol}}^{32}$ and $\mathrm{CTDI}_{\mathrm{vol}}^{16}$

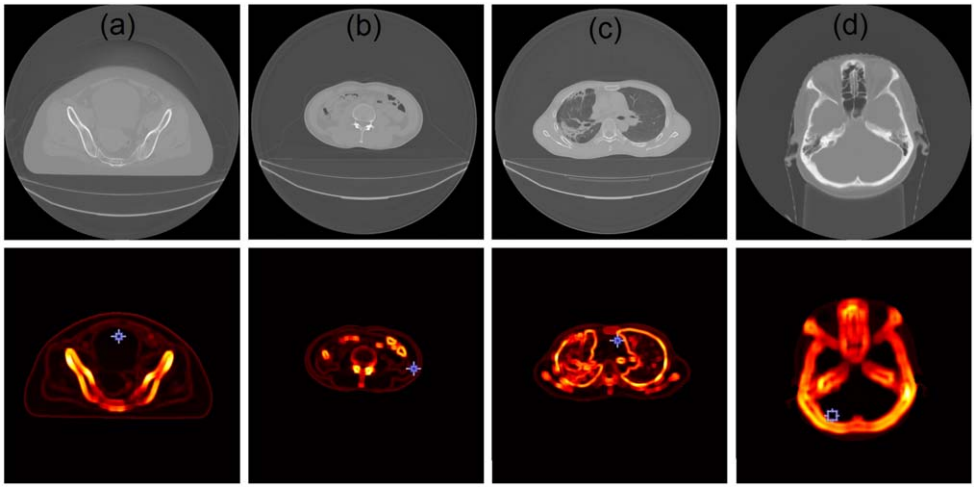

Figure 3. Original images (first row) and their corresponding standard deviation maps (second row). The blue boxes indicate the location of the smallest standard deviation which characterizes the noise of the image. (a) Pelvis, (b) abdomen, (c) thorax, and (d) head.

values were taken from the Digital Imaging and Communications in Medicine (DICOM) header.

2.3. Algorithm of automated noise calculation

Noise is generally determined by calculating the standard deviation within a homogeneous area in the ROI [34, 35]. Automated noise calculations require this be done automatically. However, the determination of a ROI in a patient is not trivial. Recently, Christianson *et al* [28] introduced an automated noise calculation algorithm without ROI detection. However, it was only able to be applied in abdominal images. Anam *et al* [28] developed a refinement algorithm that is applied to all body regions. Automated noise calculation was measured in the most homogeneous area, i.e. it was identified as the smallest standard deviation (SD) in the standard deviation map. The standard deviation map was calculated using a sliding window with kernel size of about 1 cm^2. Figure 3 shows the original images of patients (first row) and its corresponding noise maps and locations of the smallest SD in the SD map to decide the noise of the image (second row).

3. Results

The SSDE levels for the pelvis, abdomen, thorax and head of the patients as a function of Dw are shown in figure 4. The SSDE values increase linearly with increasing Dw in the pelvis, abdomen, and thorax images. The R^2 are 0.74, 0.54 and 0.82 for pelvis, abdomen and thorax, respectively. A different trend is observed in the head images, the SSDE exponentially decreases with increasing Dw. The noise for the pelvis, abdomen, thorax and head of the patients as a function of Dw are superimposed in figure 5. The noise in the pelvis, abdomen, thorax, and head images are rather constant (with R^2 around 0.01) for varying Dw.

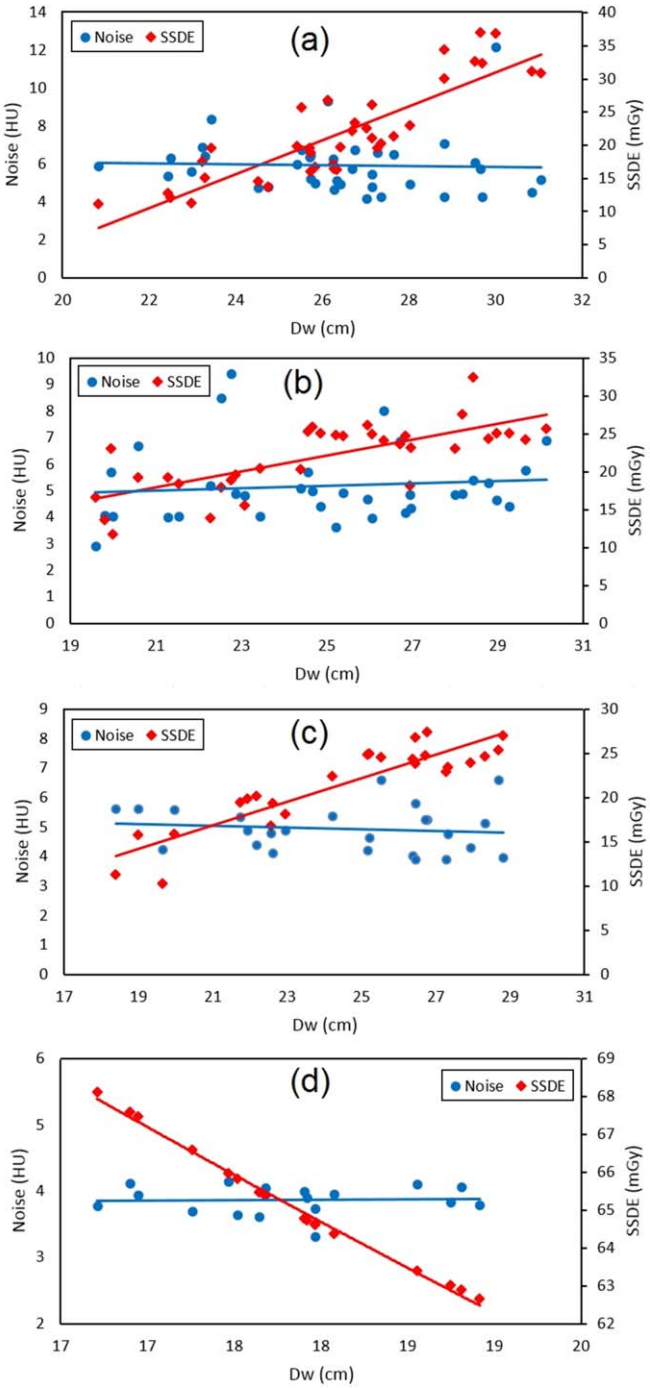

Figure 4. The result of automated noise and SSDE calculations as a function of Dw for different body parts. (a) Pelvis, (b) abdomen, (c) thorax, and (d) head.

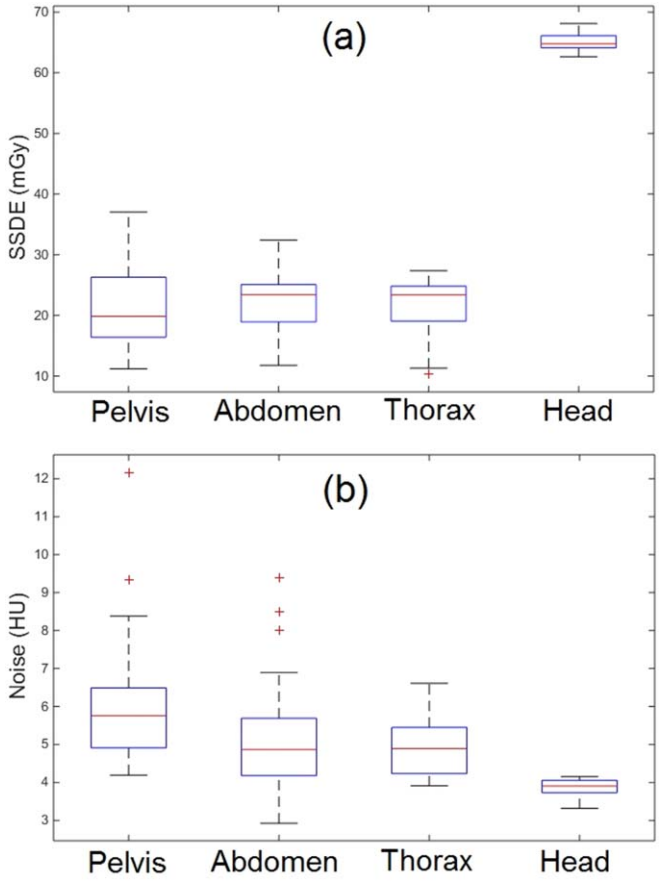

Figure 5. Box plots for different body parts. (a) SSDE, and (b) Noise.

Box plots of SSDE and noise are shown in figure 5. The SSDE values in the head image (65.1 ± 1.7 mGy) are significantly higher than for the pelvis (21.8 ± 7.3 mGy), abdomen (22.0 ± 4.5 mGy) and thorax (21.5 ± 4.7 mGy). The noise in the pelvis, abdomen and thorax images are similar with mean values of 5.9 ± 1.5 HU, 5.2 ± 1.4 HU and 4.9 ± 0.8 HU, respectively, while in the head images the noise is significantly lower at 3.9 ± 0.2 HU.

4. Discussion

The automated noise calculation [27, 28] in conjunction with an automated size-specific dose estimate (SSDE) [20, 24] can be used as a tool to optimize dose in accordance with the ALARA principle. An automated method more objectively and effectively determines the noise and SSDE than the manual method. The determination of noise is strongly influenced by the selection of the ROI by the observer, who may sometimes determines noise in an area that is not the most homogeneous.

It is found that the noise in the pelvis, abdomen and thorax images are relatively constant for varying Dw because of TCM [36–38]. Even though it did not use TCM, the noise in the

head image is also relatively constant, due to very small Dw variations in the head, of about 2 cm. This small variation of Dw leads to only a slight impact on the noise on the head.

SSDE is affected by both values of CTDIvol and size-correction factor. SSDE decreases with size in the head due to constant mA (or fixed tube current, FTC). The constant mA leads to a constant CTDIvol. This constant CTDIvol then results in a decreasing of SSDE, because of the decrease in size-correction factor. Conversely, the other examinations use tube current modulation (TCM) for dose reduction in small patients, where the mA increases with the size. This increase of mA leads to an increase in CTDIvol. If the size increases, the CTDIvol increases but the size-correction factor decreases. The combination of the increase of CTDIvol and a decrease of size correction factor can lead SSDE to remain constant, or increase, or decrease depending on which one is more dominant. This dominance depends on the magnitude of TCM. In this study, the increase in CTDIvol was more dominant than the decrease in size-correction factor, consequently SSDE increased with the size. In previous studies the reported difference in results depended on the magnitude of TCM. One study reported that the TCM technique caused a relatively constant SSDE [39], although other study reported that the TCM technique caused an increase in SSDE [40].

The current study found that the SSDE of the head was in the order of 65 mGy, a much higher dose level than other body parts examined which had SSDE values of about 20 mGy. Our results are comparable with a survey of output dose values of about 60 mGy for head CT examinations and of about 20 mGy for body examination in the US in the period 1999–2001 [41]. In this study, we found that the noise in head images was about 3.9 HU and it was lower than that in pelvis, abdominal and thorax images (about 5–6 HU). This finding indicated that the protocol for head CT examination produces too high a dose and too low noise, the dose could be further reduced while maintaining diagnostic image quality. Previously, Tipnis *et al* [42] reported that a decrease in output dose from 75 to 60 mGy in head CT examinations produced no clear degradations in depicting neuroanatomy. Based on this finding, the noise in the head image could be further increased up to about 5 HU which may be obtained with a dose lower than 60 mGy.

Comparison of doses on each examination for optimization purposes could also be conducted. In the pelvis and abdominal examination, there are several noise outliers, i.e. the noise is much greater than the average noise value for the certain examination. This phenomenon indicates that in one examination further optimization needs to be carried out. The ranges of noise values in the pelvis, abdominal and thoracic examinations are relatively large at around 4 HU, indicating that TCM optimization needs to be increased so that the dose and noise ranges can be reduced to around 2 HU. This task is challenging because the pelvis, abdomen, and thorax have relatively large variations in size, geometry and composition. A noise range of less than 2 HU has been achieved on head examinations due to the relatively small variation in head size from one patient to another, which is in the range of 2 cm.

In the current study, however, the calculated noise level has not been compared with visual observations by expert radiologists [42]. In a follow-up study, we will compare quantitative noise levels from automated methods with qualitative radiological observations determined by a radiologist. Image quality is not only characterized by noise. For a more comprehensive optimization we need to evaluate an automatic approach taking into account other measures of image quality, such as spatial resolution [43], artifacts and so on.

5. Conclusions

Implementation of automated noise calculation, along with automated size-specific estimation, may provide a convenient tool for optimizing patient doses according to the ALARA

principle. We found that the noise in head images was lower than that in pelvic, abdominal and thoracic images, while the dose in the head was about three times that in the other regions. This finding revealed that the protocol for head CT seems to be characterized by higher dose and lower noise, both of which could be further optimized while maintaining diagnostic image quality.

Acknowledgments

This work was funded by the Riset Publikasi Internasional Bereputasi Tinggi (RPIBT) 2019, Universitas Diponegoro (Contract Number: 329-116/UN7.P4.3/PP/2019). The authors give special thanks to Sanggam Ramantisan for providing images of the patients.

ORCID iDs

Choirul Anam https://orcid.org/0000-0003-0156-6797
Heri Sutanto https://orcid.org/0000-0003-3404-0337

References

[1] Voress M 2007 The increasing use of CT and its risks *Radiol. Technol.* **79** 186–90
[2] Mettler F A Jr *et al* 2009 Radiologic and nuclear medicine studies in the United States and worldwide: frequency, radiation dose, and comparison with other radiation sources–1950-2007 *Radiology* **253** 520–31
[3] Brenner D J and Hall E J 2007 Computed tomography—an increasing source of radiation exposure *N. Engl. J. Med.* **357** 2277–84
[4] Kalender W A 2014 Dose in x-ray computed tomography *Phys. Med. Biol.* **59** R129–50
[5] NCRP 2009 Ionizing radiation exposure of the population of the United States *NCRP Report* 160 Bethesda MD
[6] Pearce M S *et al* 2012 Radiation exposure from CT scans in childhood and subsequent risk of leukaemia and brain tumours: a retrospective cohort study *Lancet* **380** 499–505
[7] Miglioretti D L *et al* 2013 Pediatric computed tomography and associated radiation exposure and estimated cancer risk *JAMA Pediatr.* **167** 700–7
[8] Kalra M K *et al* 2004 Strategies for CT radiation dose optimization *Radiology* **230** 619–28
[9] Shah N B and Platt S L 2018 ALARA: is there a cause for alarm? Reducing radiation risks from computed tomography scanning in children *Curr. Opin. Pediatr.* **20** 243–7
[10] Larson D B 2014 Optimizing CT radiation dose based on patient size and image quality: the size-specific dose estimate method *Pediatr. Radiol.* **44** S501–5
[11] Karmazyn B, Liang Y, Klahr P and Jennings S G 2013 Effect of tube voltage on CT noise levels in different phantom sizes *Am. J. Roentgenol.* **200** 1001–5
[12] Spampinato M V, Stalcup S, Matheus M G, Byington K, Tyler M, Bickley S and Tipnis S 2018 Radiation dose and image quality in pediatric head CT *Rad. Prot. Dosim.* **182** 310–6
[13] Khoramian D, Sistani S and Firouzjah R A 2019 Assessment and comparison of radiation dose and image quality in multi-detector CT scanners in non-contrast head and neck examinations *Pol. J. Radiol.* **84** e61–7
[14] Anam C, Fujibuchi T, Haryanto F, Widita R, Arif I and Dougherty G 2019 An evaluation of computed tomography dose index measurements using a pencil ionisation chamber and small detectors *J. Radiol. Prot.* **39** 112–24
[15] Larson D B, Wang L L, Podberesky D J and Goske M J 2013 System for verifiable CT radiation dose optimization based on image quality: I. Optimization model *Radiology* **269** 167–76
[16] Boone J *et al* 2011 Size-specific dose estimates (SSDE) in pediatric and adult body CT examinations *AAPM Report No. 204* http://aapm.org/pubs/reports/RPT_204.pdf (Accessed: 2 March 2014)

[17] Wang J, Christner J A, Duan Y, Leng S, Yu L and McCollough C H 2012 Attenuation-based estimation of patient size for the purpose of size specific dose estimation in CT. II. Implementation on abdomen and thorax phantoms using cross sectional CT images and scanned projection radiograph images *Med. Phys.* **39** 6772–8
[18] Boos J *et al* 2016 Does body mass index outperform body weight as a surrogate parameter in the calculation of size-specific dose estimates in adult body CT? *Br. J. Radiol.* **89** 20150734
[19] Anam C, Haryanto F, Widita R, Arif I, Dougherty G and McLean D 2017 The impact of patient table on size-specific dose estimate (SSDE) *Australas. Phys. Eng. Sci. Med.* **40** 153–8
[20] Christianson O, Li X, Frush D and Samei E 2012 Automated size-specific CT dose monitoring program: assessing variability in CT dose *Med. Phys.* **39** 7131–9
[21] Anam C, Haryanto F, Widita R, Arif I, Dougherty G and McLean D 2016 Estimation of eye radiation dose during nasopharyngeal CT examination for an individual patient *Information* **19** 3951–62
[22] Kidoh M *et al* 2017 Breast dose reduction for chest CT by modifying the scanning parameters based on the pre-scan size-specific dose estimate (SSDE) *Eur. Radiol.* **27** 2267–74
[23] Anam C, Fujibuchi T, Toyoda T, Sato N, Haryanto F, Widita R, Arif I and Dougherty G 2018 A simple method for calibrating pixel values of the CT localizer radiograph for calculating water-equivalent diameter and size-specific dose estimate *Radiat. Prot. Dosim.* **179** 158–68
[24] Anam C, Haryanto F, Widita R, Arif I and Dougherty G 2016 Automated calculation of water-equivalent diameter (D_W) based on AAPM task group 220 *J. Appl. Clin. Med. Phys.* **17** 320–33
[25] Dodge C T, Tamm E P, Cody D D, Liu X, Jensen C T, Wei W, Kundra V and Rong X J 2016 Performance evaluation of iterative reconstruction algorithms for achieving CT radiation dose reduction — a phantom study *J. Appl. Clin. Med. Phys.* **17** 511–31
[26] Hussain F A, Mail N, Shamy A M, Alghamdi S and Saoudi A 2016 A qualitative and quantitative analysis of radiation dose and image quality of computed tomography images using adaptive statistical iterative reconstruction *J. Appl. Clin. Med. Phys.* **17** 419–32
[27] Christianson O, Winslow J, Frush D P and Samei E 2015 Automated technique to measure noise in clinical CT examinations *Am. J. Roentgenol.* **205** W93–9
[28] Anam C, Arif I, Haryanto F, Lestari F P, Widita R, Budi W S, Sutanto H, Fujibuchi T and Dougherty G 2019 A novel method of automated noise measurement from the most homogeneous region in CT images *Biomed. Phys. Eng. Express* unpublished
[29] Nawfel R D and Young G S 2017 Measured head CT/CTA skin dose and intensive care unit patient cumulative exposure *AJNR Am. J. Neuroradiol.* **38** 455–61
[30] Sarmento S, Mendes B and Gouvêa M 2018 Automatic calculation of patient size metrics in computed tomography: what level of computational accuracy do we need? *J. Appl. Clin. Med. Phys.* **19** 218–27
[31] Anam C, Haryanto F, Widita R, Arif I and Dougherty G 2017 The size-specific dose estimate (SSDE) for truncated computed tomography images *Radiat. Prot. Dosim.* **175** 313–20
[32] Burton C S and Szczykutowicz T P 2018 Evaluation of AAPM Reports 204 and 220: estimation of effective diameter, water-equivalent diameter, and ellipticity ratios for chest, abdomen, pelvis, and head CT scans *J. Appl. Clin. Med. Phys.* **19** 228–38
[33] American Association of Physicists in Medicine 2010 The future of CT dosimetry: comprehensive methodology for the evaluation of radiation dose in x-ray computed tomography *AAPM Report No. 111* https://aapm.org/pubs/reports/RPT_111.pdf (Accessed: 15 December 2013)
[34] Primak A N, McCollough C H, Bruesewitz M R, Zhang J and Fletcher J G 2006 Relationship between noise, dose, and pitch in cardiac multi–detector row CT *RadioGraphics* **26** 1785–94
[35] Kamezawa H, Arimura H, Shirieda K, Kameda N and Ohki M 2016 Feasibility of patient dose reduction based on various noise suppression filters for cone-beam computed tomography in an image-guided patient positioning system *Phys. Med. Biol.* **61** 3609–36
[36] Favazza C P, Yu L, Leng S, Kofler J M and McCollough C H 2015 Automatic exposure control systems designed to maintain constant image noise: effects on computed tomography dose and noise relative to clinically accepted technique charts *J. Comput. Assist. Tomogr.* **39** 437–42
[37] Angel E 2009 Monte Carlo simulations to assess the effects of tube current modulation on breast dose for multidetector CT *Phys. Med. Biol.* **54** 497–512
[38] Kalender W A, Wolf H and Suess C 1999 Dose reduction in CT by anatomically adapted tube current modulation: phantom measurements *Med. Phys.* **26** 2248–53
[39] Christner J A, Braun N N, Jacobsen M C, Carter R E, Kofler J M and McCollough C H 2012 Size-specific dose estimates for adult patients at CT of the torso *Radiology* **265** 841–7

[40] Schindera S T, Nelson R C, Toth T L, Nguyen G T, Toncheva G I, DeLong D M and Yoshizumi T T 2008 Effect of patient size on radiation dose for abdominal MDCT with automatic tube current modulation: phantom study *AJR Am. J. Roentgenol.* **190** W100–5
[41] Martin C J and Huda W 2013 Intercomparison of patient CTDI surveys in three countries *Radiat. Prot. Dosim.* **153** 431–40
[42] Tipnis S, Thampy R, Rumboldt Z, Spampinato M, Matheus G and Huda W 2016 Radiation intensity (CTDIvol) and visibility of anatomical structures in head CT examinations *J. Appl. Clin. Med. Phys.* **17** 293–300
[43] Anam C, Fujibuchi T, Budi W S, Haryanto F and Dougherty G 2018 An algorithm for automated modulation transfer function measurement using an edge of a PMMA phantom: impact of field of view on spatial resolution of CT images *J. Appl. Clin. Med. Phys.* **19** 244–52